Chapter 9

General Mechanistic Classification of Oscillatory Electrochemical Systems

9.1 Introduction

The preceding chapters reported a number of experimental and theoretical studies regarding the mechanistic basis of various oscillatory electrocatalytic reaction systems such as formic acid oxidation, H_2-oxidation or IO_3^--reduction. In so doing numerous references have also been made to mechanistic studies of other oscillatory electrochemical reactions which were previously investigated by different authors [213, 71]. In fact, scanning the recent electrochemical literature an overwhelming number of new oscillatory systems has been reported including electrocrystallization, electrocatalysis and electrodissolution [31, 30, 208, 209, 216, 217, 218, 219]. Following the precept of "Ockham's razor" [220, 221] the number of explanatory hypotheses pertaining to the plethora of periodic phenomena in electrochemistry should be kept minimal; this can be achieved by a systematic categorization of individual phenomena according to universal mechanistic criteria.

The study of formic acid oxidation or IO_3^- reduction exemplified an inductive approach towards the mechanistic clarification and modeling of an oscillatory electrochemical process: After collecting sufficient chemical information on proceeding reaction steps and educts, intermediates and products, a theoretical dynamical model was formulated which was to reproduce the observed behavior qualitatively and quantitatively. Experimental dynamical features missing in an early stage of modeling are then sought to be captured by incorporation of, for instance, additional chemical steps into the model on a basis of trial and error. This approach, though eventually successful in most cases, turns out to be rather time-consuming, since the initial formulation and subsequent modifications of the initial model towards a better qualitative and quantitative match with experiments is not based on dynamical aspects. An alternative approach towards a rapid clarification of an electrochemical oscillator consists in the initial categorization of the oscillatory system and its species with

respect to dynamical and mechanistic features such as time scales, feedbacks, mechanistic roles etc. Each oscillator category represents a class of prototype models as well as necessary mechanistic ingredients which can subsequently be searched for in the experimental system; at the same time, each category also rules out certain other model types which need not be further considered. Even though the categories do not specify detailed chemical steps, the latter approach greatly reduces the time for establishing a reasonable oscillatory electrochemical model, as necessary mechanistic features can immediately be formulated and a rather direct targeting of appropriate chemical features refining the model becomes possible.

In what aims to be the a comprehensive categorization of electrochemical oscillatory phenomena, the current chapter will join together relevant experimental and theoretical information concerning the mechanistic requirements for electrochemical oscillations. The classification scheme seeks to provide a framework where all experimental electrochemical oscillators known sofar can be included; the scheme also includes oscillatory model classes for which experimental systems are still missing.

In addition to a classification scheme, this chapter suggests a systematic operational experimental method for the stepwise categorization of an unknown oscillator. Emphasis was placed on ready experimental feasibility of the tests used as well as on the use of minimal, a priori knowledge of the electrochemical oscillator under investigation.

For electrochemical systems, Woitowicz [15] came up first with a crude, but crucial distinction between chemical and electrochemical oscillatory systems. Later, Koper extended this scheme emphasizing the crucial role of a negative differential resistance (NDR) for electrochemical instabilities. Koper [74, 23] distinguished three classes of electrochemical oscillators: first, current oscillators which oscillate under truly potentiostatic conditions, second, oscillators which oscillate only under potentiostatic conditions in the presence of an external resistance and, third, systems which oscillate under both potentiostatic and galvanostatic conditions. The present categorization scheme in principle builds on Koper's approach, however provides crucial extensions and refinements.

Note that the present classification throughout refers to oscillatory interfacial processes which are investigated in a conventional potential/current-controlled arrangement. In the literature, however, a great number of electrochemical oscillator have been reported which apparently do not require any controlled outer conditions (open circuit oscillators [1, 222, 223, 224, 225, 226, 219]). It has long been known that this is simply because the function of, for instance, a galvanostat as a constant sink/source of electrons has been taken over by a second redox system ("internal galvanostat" [225]). Consequently, the dynamical behavior of either half cell (redox system) of an open circuit oscillator can be investigated separately in the usual controlled arrangement.

The chapter is organized as follows: After a short compilation of the relevant mechanistic concepts necessary for a ready understanding of the classification, is followed by a detailed characterization of the four principal oscillator classes. Finally, the operational experimental classification procedure is described, before a short discussion concludes the chapter.

9.2 Mechanistic notions and experimental tools for classification

Most of the mechanistic concepts mentioned here have been used individually during this thesis. However, as this chapter is to culminate in a comprehensive compilation of mechanistic knowledge on electrochemical oscillators it seems appropriate to briefly put together and review those mechanistic ingredients which are crucial for the categorization of oscillatory electrochemical mechanisms.

Essential species. All modeling of electrochemical reaction dynamics throughout this thesis tacitly implied the possibility to subdivide the time-dependent chemical variables (species) or electrical variables (pseudospecies) into essential ones, meaning quantities the time dependence of which is an indispensable part of the overall reaction dynamics, and non-essential ones. Non-essential variables may also be time-dependent, but there is an experimental limiting case where these variables can be kept constant without altering the system dynamics [33]. Usually, upon investigating an unknown electrochemical system, a chemist can immediately make educated guesses as to good candidates for essential species. In modeling electrochemical behavior by means of differential equations, non-essential species can be left out as they can be included in the chemical rate constants.

Feedback loops. The essential species, in turn, can usually be subdivided according to their time scale. In the complex electrochemical mechanisms considered here some variables are usually fast, whereas others are slow. For non-trivial dynamics such as multistability, sustained oscillations or excitability to occur both fast and slow variables have to lie on mechanistic feedback loops. One loop must contain fast variables only, while a second loop must contain at least one slow variable in addition to at least one of the fast ones. The former feedback loop is the positive destabilizing loop, whereas the latter is referred to as negative stabilizing feedback loop (see chapter 5).

Current Carriers. In chapter 5, 7 and 8 the notion of an dependent and independent current carrier (current providing reaction) has been introduced. The distinction and rigorous definition of these two types of charge transfer reaction is closely linked to the concept of essential and non-essential species: dependent current carriers consume the slow, inhibiting essential species or any intermediate formed from the slow species and may, on top, be dependent on fast variables; in contrast, independent current carriers consume non-essential (pseudo)species only. Note that the indication of a time scale is irrelevant for non-essential species. An example of a dependent current carrier is the reduction of the slow IO_3^- ions (chapter 8), while the diffusion limited H_2 oxidation current in chapter 7 represents an independent current carrier. The application of the notion of dependent and independent current carriers greatly simplifies a rapid categorization of electrochemical oscillators.

Voltammetry and impedance behavior. Basic information about an electrochemical process is provided by the stationary voltammetric profile of the current providing reaction, i.e. the profile of the faradaic current. In the simplest case only one reaction is electrochemical. Figure 9-1 sketches the principal types of non-trivial stationary I/ϕ curves occurring in electrochemical oscillators (cf.[227]). Note that stability of

the voltammetric branches has been neglected. The striking feature of all of them consists in at least one potential region with a negative differential resistance (NDR), which, as seen in chapter 4, 5,7 and 8 is immediately linked to many experimental electrochemical instabilities described in the literature sofar. In can happen, though, ("HNDR" oscillators), that the negative differential resistance may only be visible on a fast time scale. Still, as will be shown theoretically in the next section, unlike previous conjectures [26] one should be cautious when judging from the shape of the I/ϕ curve alone, whether an observed NDR is linked to the relevant experimental instability.

In upcoming sections, it will also be investigated whether the impedance spectrum of an experimental oscillator rigorously represents a sufficient criterion for a mechanistic categorization as was suggested in ref. [74, 23]. To this end the impedance spectra of simple electrochemical oscillators will be modelled. Following chapter 2, the admittance of an electrochemical process involving potential and one chemical variable $\dot{\theta} = f(\theta, \phi)$ is easily calculated as

$$Z^{-1} = \frac{\partial I_f}{\partial \phi} + \frac{\partial I_f}{\partial \theta}\frac{\Delta\theta}{\Delta\phi} \tag{9.1}$$

where

$$\frac{\Delta\theta}{\Delta\phi} = \frac{-\frac{\partial f}{\partial \phi}\frac{\partial f}{\partial \theta}}{\omega^2 + \frac{\partial f}{\partial \theta}^2} - i\frac{\frac{\partial f}{\partial \phi}\omega}{\omega^2 + \frac{\partial f}{\partial \theta}^2} \tag{9.2}$$

All partial derivatives are evaluated at the stationary state. Note that in eq. 9.2 the impedance spectrum is a combination of all four Jacobian elements and does not allow the distinction of their individual signs. This will become of importance when different oscillator classes will be identified by feedback control methods which, as chapter 7 showed, allow conclusions as to the sign of individual Jacobi matrix elements.

An upcoming section will deal with a systematic operational procedure for the classification of an unknown electrochemical oscillator. The experimental tools used during this categorization procedure include both conventional electrochemical techniques and non-standard tests especially designed for a mechanistic reconnaissance of oscillatory systems. In particular, the tools include

- potentiostatic and galvanostatic I/U curves for the assessment of the stationary polarization behavior
- measuring the bifurcation behavior (Hopf bifurcation (HB), and saddle-node bifurcation) with respect to their relative location at constant external resistance R ; moreover, the shape of the bifurcation diagram in the U-R plane
- potentiostatic and galvanostatic impedance measurements for the investigation of the dynamics on varying time scales
- feedback control tests ($\dot{I}/U$, $\dot{\theta}/U, \dot{\theta}/I$) for the assessment of the mechanistic

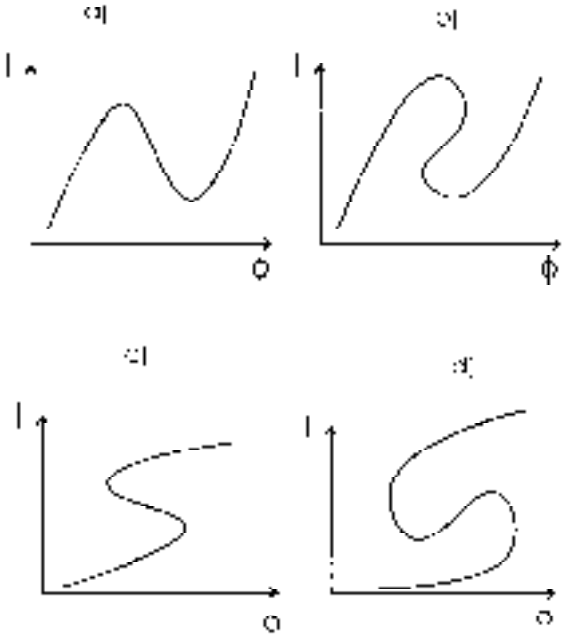

Figure 9-1: Common types of stationary current/potential curves at vanishing ohmic resistance R occuring in electrochemical oscillators. Stability of the stationary points is not explicitly indicated. a) simple N (may be hidden on a fast time scale), b) complex N, c) simple S, d) complex S

role of certain species as well as for the direct investigation of the signs of the Jacobian matrix.

9.3 Principal mechanistic classes of electrochemical oscillators and their experimental characteristics

In ref. [74], Koper suggests a mechanistic categorization of electrochemical oscillators based on the experimental control mode and impedance spectra. All oscillatory mechanisms considered by Koper included at least one autocatalytic (pseudo)species. The present categorization scheme elaborates on Koper's suggestions (i) by using mechanistic criteria rather than experimental conditions for the distinction of oscillatory categories (ii) by extending the classification by an additional principal oscillator class (iii) by a detailed investigation of purely potentiostatic oscillators [74] and (iv) by the identification and characterization of frequently occurring oscillatory subclasses. The current section also tries to sketch the qualitative experimental behavior of the

respective oscillator classes when encountered in experiments. The present classification pertains to electrochemical oscillators containing at least one autocatalysis. Thus, the group of oscillatory models intentionally left out here is the highly exotic class of nonautocatalytic oscillators [228] which are theoretically conceivable, yet rather irrelevant until an experimental system of this type is identified.

The distinction of the principal oscillatory categories refers to the mechanistic role of the double layer potential ϕ in the presence of at least one autocatalysis. The scheme includes

- Class I, where ϕ is nonessential, while both the autocatalysis and the slow species are purely chemical
- Class II, where ϕ is the essential slow variable with the autocatalysis still chemical
- Class III and VI, where ϕ is autocatalytic, with a chemical species forming the slow, negative feedback. Despite the common features both categories exhibit very distinct dynamical behavior.

9.3.1 Class I: strictly potentiostatic oscillators

Mechanistic features

Strictly potentiostatic oscillators essentially represent purely chemical oscillators involving at least one electrochemical step, i.e. one chemical reaction is associated with charge-transfer at an electrode interface. The instability of these oscillators is not of electrical nature. The interfacial potential drop ϕ is nonessential and in principle need therefore not be considered in dynamical modeling of the dominating instability. Consequently, it is a crucial feature of class I oscillators that current oscillations persist even in the experimental limiting case of vanishing external resistance R where ϕ remains constant and can be regarded as parameter. Yet for finite R, ϕ becomes time dependent and may even be part of a nonessential positive feedback loop. For class I oscillators in principle all I/ϕ characteristics of Fig. 9-1 are observable.

As pointed out in ref. [74], the instability (positive feedback) can be either based on deviations from ideal Langmuir adsorption as well as an adsorbate-induced surface phase transitions (leading to S and complex S shaped voltammetric curves) or may be due to a kinetic (synergistic or competitive) autocatalysis involving one or more species (leading to N or S shaped curves as shown below). A detailed classification of chemical oscillators with synergistic autocatalysis was put forward by Eiswirth et al. [33] who started from a marginally stable autocatalytic model and distinguished mechanistic oscillatory classes according to the modifications necessary to obtain an exponentially unstable model. Modifications regarding the stoichiometry and the kinetics of the initial autocatalysis led to oscillators of type 1 and 2, respectively. While type 1 oscillators always exhibit a XPD in some two-parameter plane, it is characteristic for type 2 oscillators to never display a XPD.

The dynamics of simple models of class I oscillators

In order to illustrate the versatile dynamics of oscillators of class I in more detail, an originally chemical type-2 oscillator model was studied numerically with one chemical step being associated with charge transfer. The oscillator used is the well-known Brusselator [229] and reads

$$A \rightleftharpoons X \tag{9.3}$$
$$2X + Z \rightharpoonup 3X \tag{9.4}$$
$$X \rightharpoonup Z \tag{9.5}$$
$$Z \rightharpoonup P \tag{9.6}$$

Its network diagram is given in Fig. 9-2. A and P are nonessential, while X is the essential autocatalytic species and X and Z form a negative, stabilizing two-loop. The time evolution of species X and Z in dimensionless variables is given by the two differential equations

$$\dot{x} = a - x - b\ x + x^2 z \tag{9.7}$$
$$\dot{z} = -x^2 z + b\ x - c\ z \tag{9.8}$$

with a,b and c denoting rate constants.

Charge transfer in the negative feedback loop. First, reaction step 9.5 is assumed to be an anodic electrochemical process with the Butler-Volmer rate expression being Taylor-expanded to first order (see bold arrow in Fig. 9-2). The resulting dimensionless electrochemical system reads

$$\dot{x} = a - x - (b + \phi)x + x^2 z \tag{9.9}$$
$$\dot{z} = -x^2 z + (b + \phi)x - cz \tag{9.10}$$
$$\epsilon\dot{\phi} = \frac{U_{ex} - \phi}{R_{ex}} - (b + \phi)x \tag{9.11}$$

where ε, U_{ex} and R_{ex} denote the relative time scale of ϕ, the applied outer potential and the dimensionless product of ohmic series resistance (solution and external circuit) and electrode area, respectively. While for $R_{ex} > 0$ the total current is given by $j_{tot} = \frac{U_{ex}-\phi}{R_{ex}}$, at $R_{ex} \to 0$ (strictly potentiostatic case) the relation $j_{tot} = (b+\phi)x$ holds true as the third equations disappears.

The associated Jacobian sign matrix of the electrochemical model evaluated at an unstable focus near the HB reads

$$\begin{pmatrix} + & + & - \\ - & - & + \\ - & 0 & - \end{pmatrix}$$

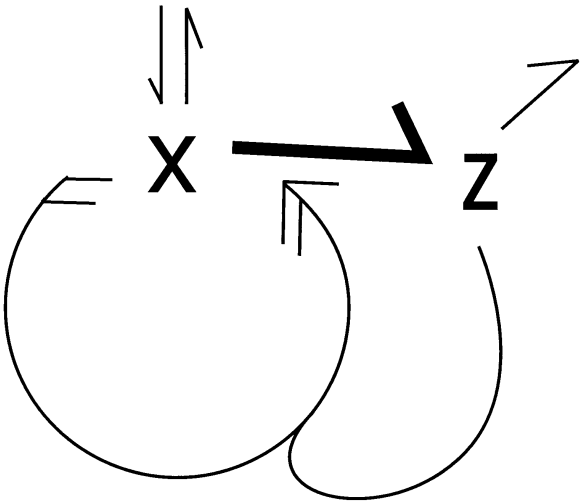

Figure 9-2: Stochiometric network diagram of a Class I (strictly potentiostatic) oscillator with a non-autocatalytic electrochemical reaction (thick solid line) illustrated by means of a model of an 'electrochemical Brusselator': Arrows connecting species symbolize chemical reactions; total number of feathers and barbs at a species denote its stochiometric coefficients as educt and respectively product (no feathers denotes a stoichiometry and kinetic coefficient equal to 1); number of left feathers encode the kinetic coefficient of the species.

indicating - apart from the dominating 2x2 unstable subsystem in X and Z - a positive two-loop between ϕ and X as well as a negative three-loop.

The potentiostatic I/ϕ behavior at vanishing R_{ex} shown in Fig. 9-3 displays a complex N shaped curve with the supercritical HB located on a branch of positive slope. Similar to findings in experimental oscillatory systems such as formic acid oxidation (which is *not* a class I oscillator, though) the HB moves to lower values of I and ϕ as R_{ex} is increased. The bifurcation diagram in the $U_{ex} - R_{ex}$ plane of the electrochemical model is given in Fig. 9-4. At $R_{ex} \to 0$, the supercritical HB is located cathodically of the saddle-node bifurcations. For increasing R_{ex}, the HB point is seen to move to anodic potentials with respect to the lower saddle-node bifurcation eventually turning into a subcritial HB beyond some critical R_{ex}. Still, as R approaches infinity the HB survives enabling galvanostatic potential oscillations (the galvanostatic HB becomes supercritical for slightly lower values of a). In the galvanostatic mode, the HB point has reached its most cathodic location along the stationary complex N-shaped curve of Fig. 9-3. Obviously, the imposition of a constant (or nearly constant, depending on the time scale of ϕ) reaction rate does not suppress sustained potential oscillations. Figure 9-3 also displays the calculated faradaic impedance spectra at two potentials along the voltammetric profile (1,2). Spectrum 1 exhibits

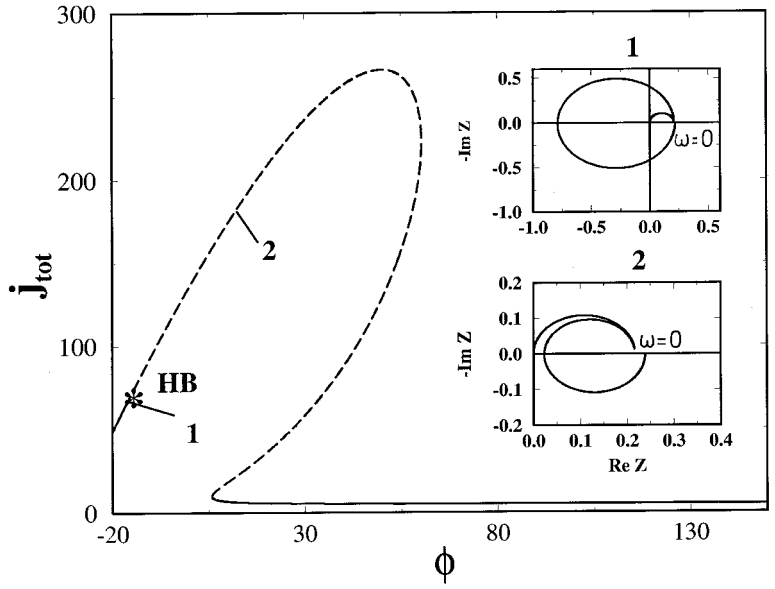

Figure 9-3: Stationary I/ϕ behavior of class I oscillator eq. 9.9 to 9.11 for $R_{ex} \to 0$ (strictly potentiostatic case); solid and dashed curve symbolize stable and unstable stationary states, respectively. HB denotes a Hopf bifurcation point. Insets 1 and 2: impedance spectra at the respective stationary states. Parameter used: $a = 5, b = 30, c = 0,07, \epsilon = 1$.

a negative differential resistance, which is hidden on a fast time scale. Importantly, this indicates the formally autocatalytic nature of ϕ at these parameters due to the positive two-loop seen in the Jacobian, but would be misleading when determining the dominant dynamical instability. This is why the impedance spectrum in itself is insufficient to uniquely distinguish an oscillator's mechanistic category as suggested in ref. [74]. Finally, Fig. 9-5 schematically depicts the experimental voltammetric behavior at sufficient low scan rates under potentiostatic (small R_{ex}) and galvanostatic conditions. The grey-shaded areas indicate the oscillatory regions (small-amplitude side near HB), while the arrows denote discontinuous current (or potential) jumps where either the stable polarization branches or stable oscillations disappear.

Charge transfer in the positive feedback loop. Next, reaction step 9.4 of the Brusselator is assumed to be associated with charge transfer (see Fig. 9-6). After introduction of an additional equation for the charge balance of the system and Taylor expansion of the Butler-Volmer terms one obtains the system of evolution equations

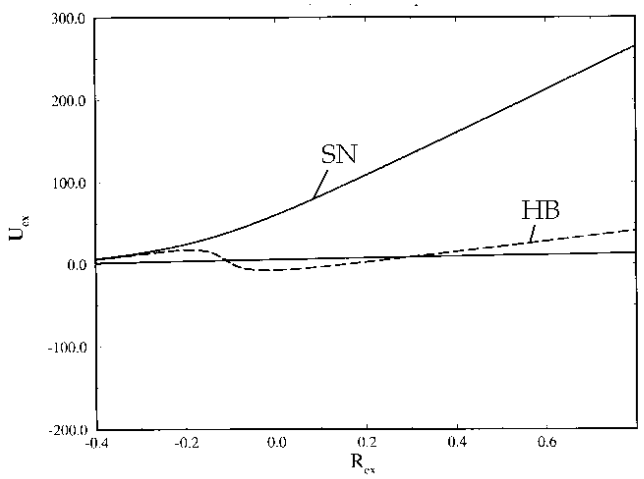

Figure 9-4: Two-parameter bifurcation diagram for the electrochemical oscillator, eq. 9.9 to 9.11. Parameters as in previous figure.

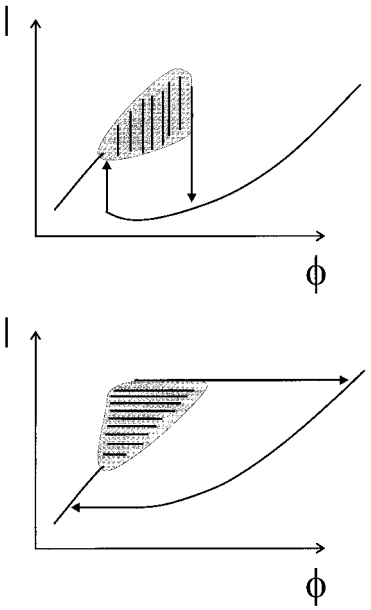

Figure 9-5: Schematic voltammetric I /ϕ behavior of model eq. 9.9 to 9.11 under potentiostatic (upper) and galvanostatic (lower) conditions for R→0 at finite scan rate; arrows indicate abrupt switches of the current while scanning; grey area with vertical black bars symbolizes the emergence of current spikes indicating current oscillations; height of grey area qualiatively encodes the spike amplitude.

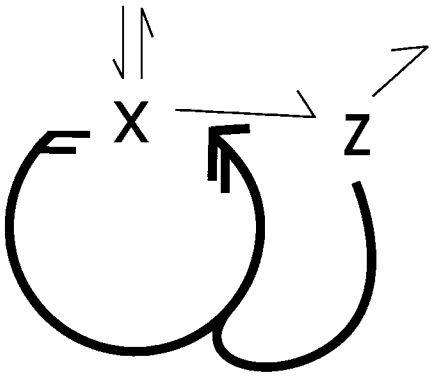

Figure 9-6: Stochiometric network diagram of a Class I (strictly potentiostatic) oscillator with an autocatalytic electrochemical reaction (thick solid line, 'electrochemical Brusslator').

$$\dot{x} = a - x - bx + (1+\phi)\, x^2 z \tag{9.12}$$

$$\dot{z} = -(1+\phi)\, x^2 z + bx - cz \tag{9.13}$$

$$\epsilon\dot{\phi} = \frac{U_{ex} - \phi}{R_{ex}} - (1+\phi)\, x^2 z \tag{9.14}$$

with the same parameters as before. Now, at $R \to 0$ (strictly potentiostatic case) $j_{tot} = (1+\phi)\, x^2 z$.

The associated Jacobian sign matrix evaluated at an unstable focus reads

$$\begin{pmatrix} + & + & + \\ - & - & - \\ - & - & - \end{pmatrix}.$$

Here, a positive two-loop exist between ϕ and Z as well as a negative one between ϕ and X; furthermore two positive three-loops are discernible.

The strictly potentiostatic voltammetric profile of the electrochemical model presents itself quite differently compared to the previous one as seen in Fig. 9-7. The overall I/ϕ curve is S -shaped with the HB on the upper branch of positive slope. Around the HB, the faradaic impedance shows a negative real part at a finite frequency and therefore hidden on a stationary curve which reflects the presence of a positive feedback loop in the Jacobian. However, as mentioned earlier, from impedance studied alone one can not draw a clear-cut conclusion as to the dominant autocatalytic variable. For increasing resistances, the HB moves to more cathodic potential. Fig. 9-8 depicts the full bifurcation behavior in the $U_{ex} - R_{ex}$ plane. In contrast to the electrochemical

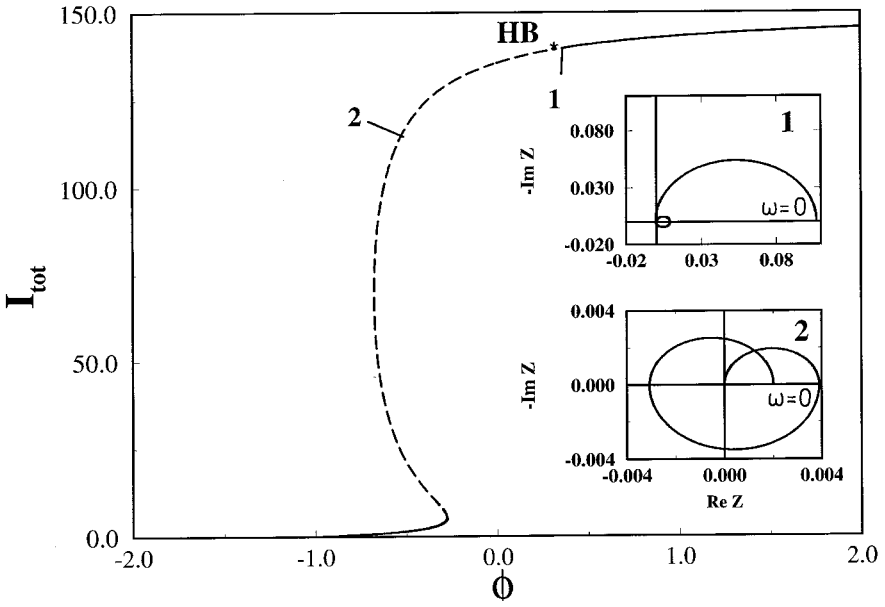

Figure 9-7: Stationary I/ϕ behavior of class I oscillator eq. 9.12 to 9.14 for $R_{ex} \rightarrow 0$ (strictly potentiostatic case); solid and dashed curve symbolize stable and unstable stationary states, respectively. HB denotes a Hopf bifurcation point. Insets 1 and 2: impedance spectra at the respective stationary states. Parameter used: $a = 5, b = 30, c = 0,07, \epsilon = 1$.

model considered above, the bistable and oscillatory regime of the present model does not extend to large values of R_{ex} suggesting the absence of galvanostatic potential oscillations. This is clearly due to the S - shaped voltammogram which gradually disappears in a cusp as the resistance increases. The absence of galvanostatic oscillations can plausibly be pictured from a more physical point of view: imposing a constant reaction rate on the rapidly varying, autocatalytic pathway constitutes a serious quenching of the destabilizing part of the mechanism leading to monostability. Obviously, the presence or absence of galvanostatic instabilities within class I provides information regarding the location of the electrochemical step. Finally, Fig. 9-9 schematically indicates how the experimental voltammogram of the electrochemical oscillator looks like at sufficiently low scan rates.

Experimental identification and characterization

Looking at the three-variable model equations discussed above the evaluation whether or not ϕ is an essential variable is not straight-forward. By definition [230, 231, 33] a nonessential species can be kept constant without qualitatively altering the oscillations in the remaining species. Obviously, for an electrochemical oscillator, the nature of ϕ can be tested potentiostatically as $R_{ex} \rightarrow 0$ what is usually performed

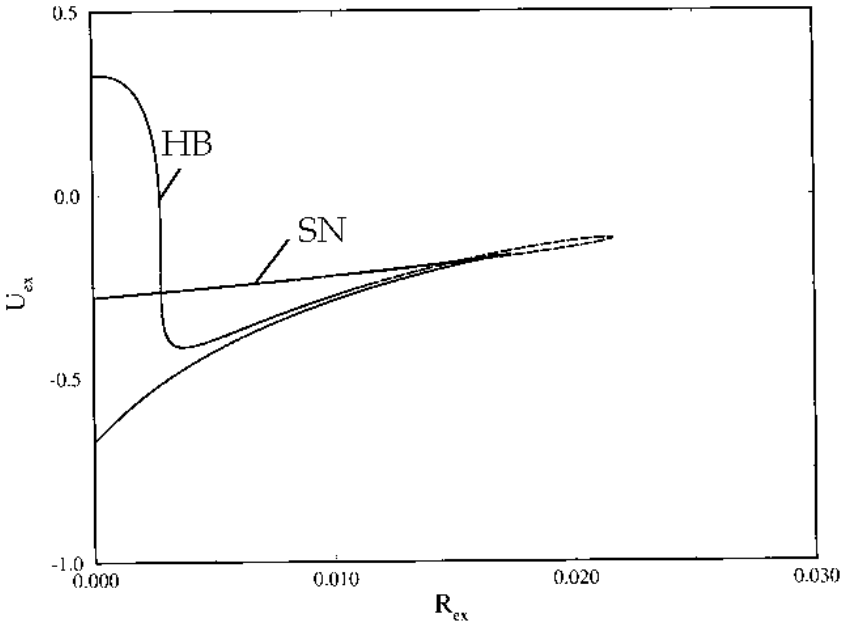

Figure 9-8: Two-parameter bifurcation diagram for the electrochemical oscillator, eq. 9.12 to 9.14. Parameters as in previous figure.

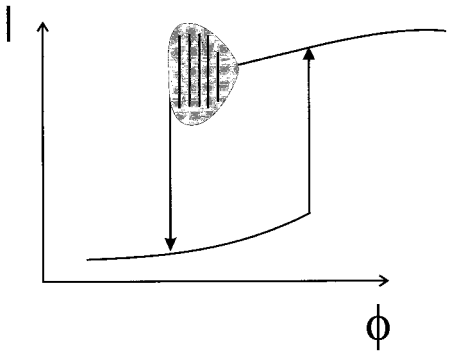

Figure 9-9: Schematic voltammetric I /ϕ behavior of model eq. 9.12 to 9.14 under potentiostatic conditions for R→0 at finite scan rate; symbols as in Fig. 9-5.

by means of a IR compensation technique. If for vanishing ohmic resistance current oscillations persist, the nonessential nature of ϕ and, therefore, the presence of a class I oscillator is demonstrated. Though experimentally easy to implement, proper functioning of the method requires a precise knowledge of the ohmic resistance.

This problem can be circumvented by using the feedback control introduced in chapter 7. There, it has been shown that - while decreasing the series resistance of solution external circuit - the successful suppression of sustained current oscillations by $\dot{I}/U$ feedback control, associated with the successful stabilization of the unstable focus, is a sufficient criterion for the presence of the limiting case where ϕ can be regarded as parameter. If, however, upon stepwise lowering R_{ex} the oscillations cease in the absence of derivative control, the system is definitely not a class I oscillator.

The galvanostatic behavior, as discussed above, can furthermore allow valuable conclusions as to the location of the charge-transfer step within the chemical network. Finally, using $\dot{\theta}/I$ or $\dot{\theta}/U$ feedback control tests the sign of the potential dependence of the rate of change of individual species, i.e. the respective off-diagonal element of the Jacobian, can be determined. This provides further mechanistic information as to the nature of the electrochemical step.

To date, there is only a very small number of experimental examples belonging to class I. First, following the scheme indicated above, there are experimental examples for class I where a purely chemical oscillator, such as the Belousov-Zhabotinskii (BZ) reaction, was modified such that an appropriate redox reaction proceeds at an electrode interface thereby inducing periodic interfacial charge-transfer [232, 233, 234]. In ref. [232] a BZ-like system ($H_2/Pt/Ce^{3+}/Ce^{4+}/BrO_3^-$) was operated without any organic oxidizable substance such as malonic acid. Instead, a reductive, electrified interface ($Pt/H_2/H^+$) took care of recovering the reduced form of the catalyst (Ce^{3+}/Ce^{4+}) and the formation of bromide. Fig. 9-10 depicts the network diagram of the mechanism. While $HBrO_2, Ce^{3+}$ as well as Br^- are essential species in the 1C oscillator [33], the 1B oscillator (exit feedback [33]) involves $HBrO_2, Br_2$ and Br^- as essential species with the electrode potential being nonessential in both cases.

On the basis of the experimental findings in ref. [105] the electrodissolution of Cu in concentrated acetic acid was identified as strictly potentiostatic oscillator (see chapter 7). There are some further systems which presumably relate to class I as their current oscillations persist to almost negligible ohmic resistances and autocatalytic chemical steps are believed to be involved. Examples are the electrodissolution of iron in highly concentrated nitric acid [67, 235], where also an complex N-shaped I/ϕ profile was found at vanishing R_{ex}, as well as the electrodissolution of silicon in fluoride media, far in the electropolishing regime [78]. Recently a strictly potentiostatic mechanisms has also been proposed for the oscillatory Fe dissolution in acidic $K_2Cr_2O_7$ solutions [219] at potentials far cathodically of the range where passivation occurs.

9.3.2 Class II: S-shaped polarization

In previous categorization approaches, little explicit attention has been paid to the present mechanistic class of electrochemical oscillators, since they appear directly

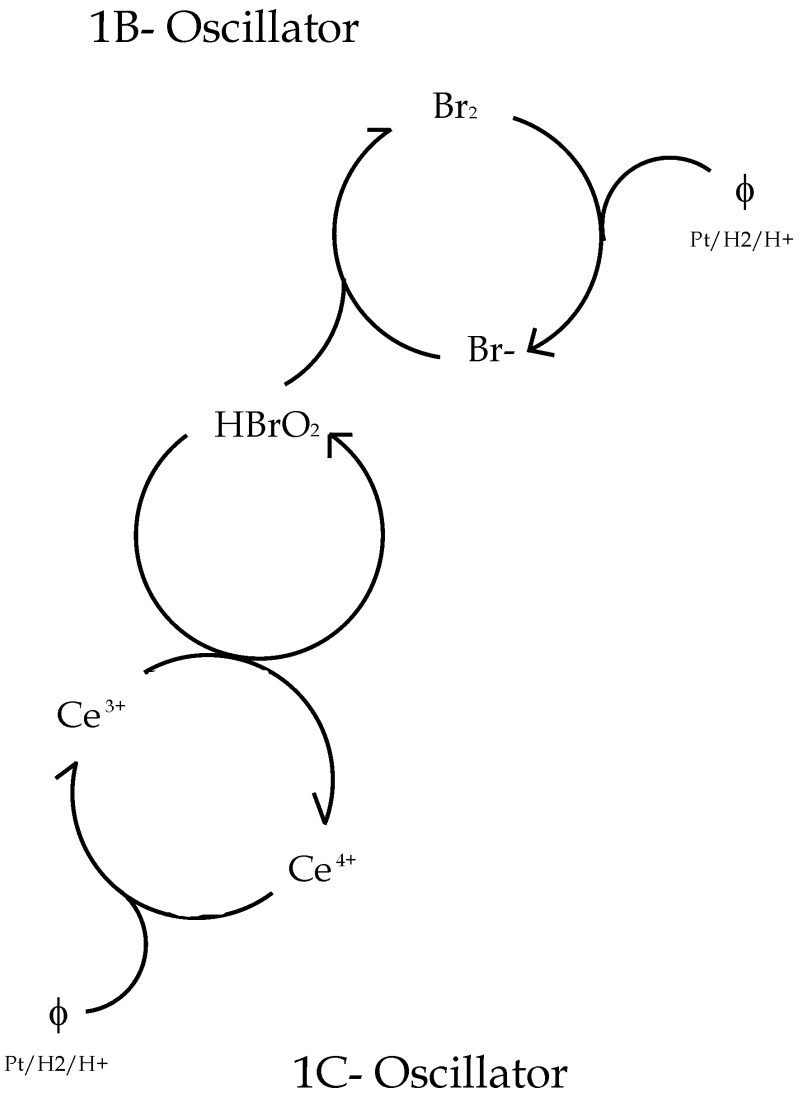

Figure 9-10: Skeleton reaction network diagram of an oscillatory BZ-like mechanism associated with the oscillatory $H_2/H^+/Pt/Ce^{3+}/Ce^{4+}/BrO_3^-$ system in the presence of a redox catalyst [232]. As the double layer potential is nonessential the oscillators belong to Class I. Other nonessential chemical species are omitted.

related to class I; yet their mechanistic features are clearly distinct from strictly potentiostatic oscillators.

Class II oscillators contain a destabilizing mechanistic feature involving only chemical species as dynamical variables. Typically, such features are potential-dependent chemical surface phase transitions between a lattice-gas like and condensed adsorption state that lead to deviations from the ideal Langmuir adsorption isotherm due to interactions of the adsorbates. Equally, any purely chemical autocatalysis involving one or more autocatalytic species and at least one charge-transfer step can provide the destabilizing mechanistic ingredient. Up to here, this looks pretty much like what has been discussed earlier. However, the crucial difference to class I oscillators is that here an appropriate chemical negative feedback loop is missing; instead, the slow, negative feedback is provided by the double layer potential ϕ being thereby an essential system variable. This is why under strictly potentiostatic conditions all oscillatory behavior ceases and merely the destabilizing chemical feature becomes visible in the stationary I/ϕ curve which usually manifests itself in a strictly potentiostatic bistable profile when the stationary coverage of an autocatalytic species is plotted vs. a system parameter. Depending on the relation between autocatalytic species and faradaic current, the bistable adsorption profile gives ideally rise to a (simple or complex) S- or a Z-shaped I/ϕ profile [227]. For obvious reasons (open circuit potential), an ideally Z-shaped voltammogram cannot exist in a real electrochemical system, but becomes distorted to a complex N- shaped curve (see Fig. 9-1). The latter profile, however, is unable to yield sustained current or potential oscillations when interacting with an external load-line (see chapter 2). Therefore, only S- shaped voltammetric curves need to be considered.

A simple dimensionless model of a typical class II oscillator describing the time evolution in the mean field of the coverage θ of a chemical species as well as of the double layer potential ϕ reads in the galvanostatic mode

$$\dot{\theta} = k_a e^{-\alpha f \phi} e^{0.5\gamma\theta}(1-\theta) - k_d e^{(1-\alpha) f \phi} e^{-0.5\gamma\theta}\theta \tag{9.15}$$

$$\epsilon\dot{\phi} = j_{tot} - e^{\alpha f \phi}(1-\theta). \tag{9.16}$$

Here, eq. 9.15 involves the ad-and desorption of a chemical species with particle interactions [236]. Furthermore, eq. 9.16 contains an anodic independent faradaic current carrier (one electron transfer) with normal potential regulation. Parameters k_a and k_d denote the ad- and desorption coefficient, α the transfer coefficient, f the electrochemical exponential factor and $\epsilon = C_{dl}/q_{mono}$ the relative time scale of ϕ (C_{dl}; double layer capacitance, q_{mono} : charge associated with a complete monolayer). The parameter γ can be interpreted as interaction parameter of the adsorbates [64, 236].

Fig. 9-11 illustrates the calculated dependence of oscillatory behavior on the relative time scale ϵ. Clearly, as long as ϕ exceeds a critical time scale, it is unable to serve as negative feedback and only bistability can be observed. For larger ϵ, however, i.e. when ϕ becomes slow, a supercritical HB bifurcates from a saddle-node curve. This reflects a practical problem often encountered when searching for class II oscillators. The electrical quantity ϕ is an inherently fast variable compared to

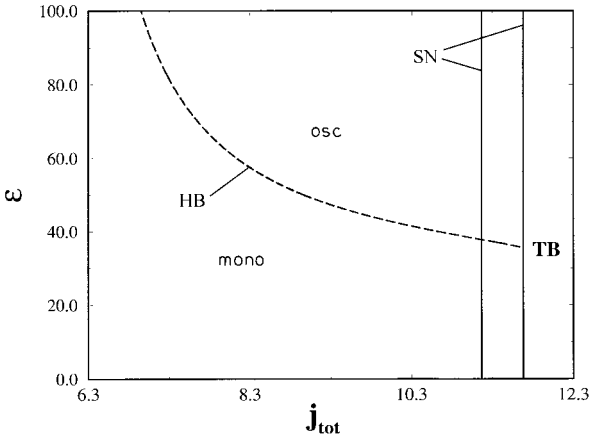

Figure 9-11: Numerical two-parameter bifurcation diagram of class II oscillator, eq. 9.15 and 9.16, under galvanoststic conditions. Dashed (solid) curves indicate the locations of Hopf (saddle-node) bifurcations. 'osc' and 'mono' indicate the parameter regions of potential oscillations and stable stationary behavior, respectively; parameter values are $k_a = 10, k_d = 1, \gamma = 8, \alpha = 0.5, f = 38.5$.

the time scale of chemical processes. Fast experimental surface phase transitions in combination with highly capacitive electrode surfaces, however, could provide an appropriate time scale for oscillations. The transition from a simple S to a complex S-shaped voltammetric profile is demonstrated in the $\gamma - j_{tot}$ bifurcation diagram (see Fig. 9-12). For medium γ $(5,5 < \gamma < 7,5)$ a simple S-shaped I/ϕ profile yields galvanostatic potential oscillations bracketed by two supercritical HB, while for large γ, the simple S deforms into a complex S shape. Fig. 9-13 shows the typical potentiostatic $U_{ex} - R_{ex}$ bifurcation diagram of class II with bistable behavior at low and oscillatory behavior at large values of the ohmic resistance. Obviously, class II oscillators never yield a XPD.

The typical, experimentally observable voltammetric behavior is schematically depicted in Fig. 9-14 for various experimental conditions. While 9-14a, c and e show the I/ϕ profile at vanishing ohmic resistance or, equivalently, under conditions where ϕ is too fast to oscillate, Fig. 9-14b, d and f displays the oscillatory regions for an appropriate ratio of time scales. Note in Fig. 9-14b,d that galvanostatic oscillations are only observable on the branch of negative slope, while potentiostatic current oscillations occur on branches with positive slope. Finally, Fig. 9-15 reproduces the characteristic impedance spectrum measured under galvanostatic conditions on the middle branch of the S- shaped profile (see black dot in 9-14).

Once a class II oscillator has been identified, $\dot{\theta}/U$ as well as $\dot{\theta}/I$ feedback control tests can be employed in order to decide whether or not the current carrier is of dependent or independent nature, i.e. whether or nor it is consuming the slow essential species.

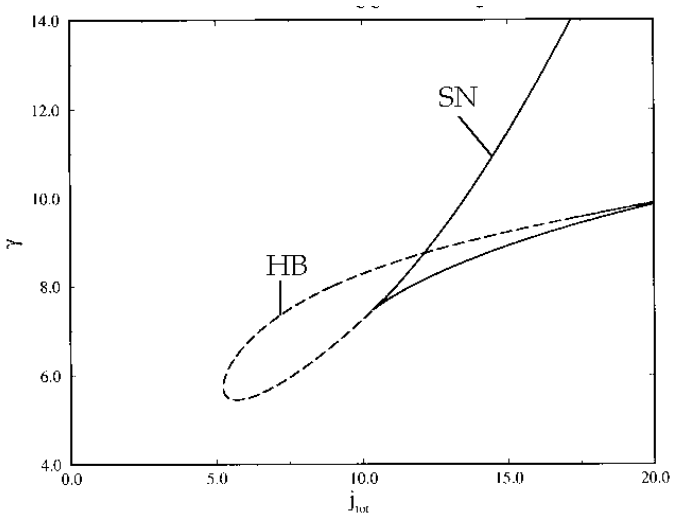

Figure 9-12: Bifurcation behavior of model eq. 9.15 and 9.16 in dependence of the interaction parameter γ and the total current j_{tot}. HB and SN denote the location of Hopf bifurcations and saddle-node bifrucation, respectively. parameters as in previous figure and $\epsilon = 50$.

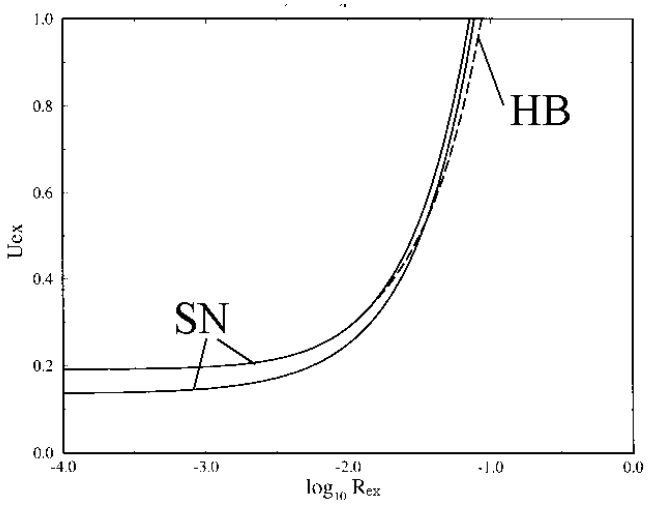

Figure 9-13: $U_{ex} - R_{ex}$ bifurcation diagram of the potentiostatic model corresponding to eq. 9.15 and 9.16. Parameters as in previous figure with $\gamma = 8$.

There are a number of electrochemical oscillatory models described in the literature which consider a coverage-dependent adsorption constant as the source of the instability [237, 238, 239, 170]. In particular, the model in ref. [170] closely resembles

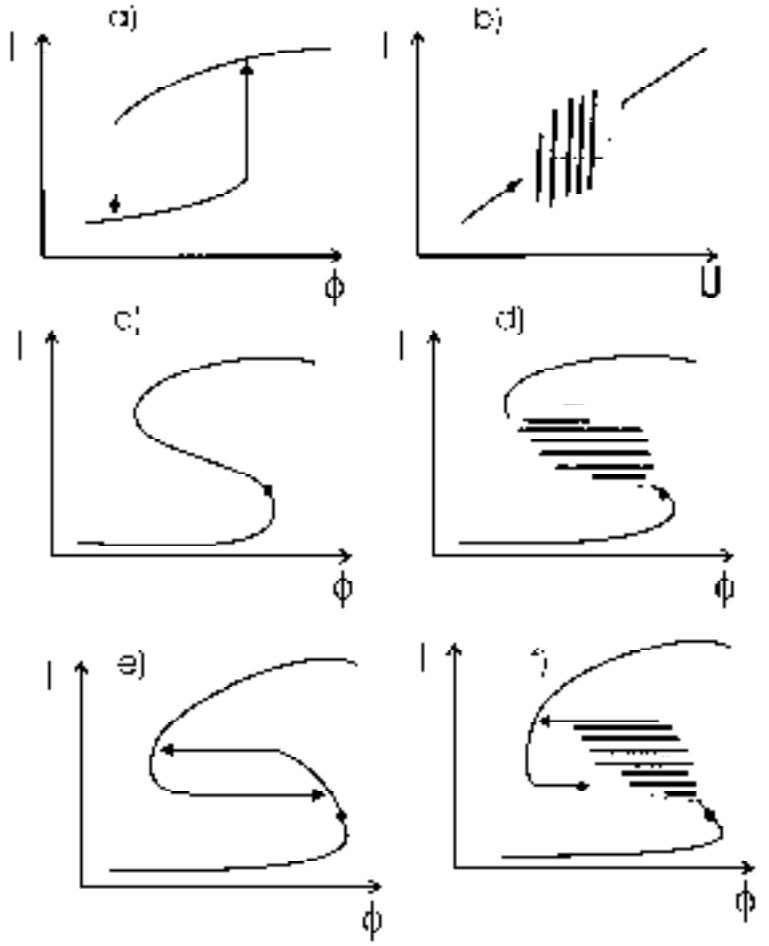

Figure 9-14: Schematic current/potential characteristics of class II oscillators. a) Strictly potentiostatic I/ϕ behavior; b) potentiostatic I/U behavior for sufficiently large value of R_{ex}; c) and d) galvanostatic I/ϕ behavior in the case of a simple S-shaped polarisation curve for subcritical and respectively supercritical value of ϵ; e) and f) galvanostatic I/ϕ behavior in the case of a complex S-shaped polarisation curve for subcritical and respectively supercritical ϵ.

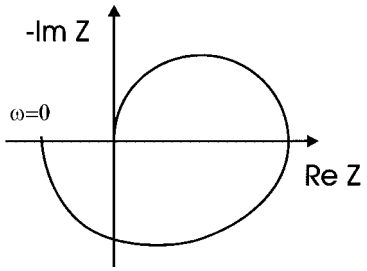

Figure 9-15: Characteristic impedance diagram of class II oscillators as obtained at the points of the current/potential curves (previous figure) indicated by the black solid circles.

the class II-prototype model considered above; unfortunately, however, the model was designed to describe potential oscillations during H_2-oxidation in the presence of metal cations which clearly do not fall in the present category [29, 74, 98]. Experimental electrochemical systems with a S- shaped I/ϕ characteristics were reported by Epelboin et al. [240] who studied the electrocrystallization of Zn. Fig. 9-16 and 9-17 reproduce the experimental findings. Here, the fast dynamics of ϕ impedes the observation of oscillations. An example for an Z shaped I/ϕ profile is the electrodissolution of Sn in alkaline media [241] where oscillations are generally absent.

In the oscillatory $H_2/H^+/Pt/BrO_3^-$ system in the absence of metal catalysts [232], the electrode potential may become a nonautocatalytic, essential variable involved in the autocatalytic formation of bromic acid (along side with the formation of Br^-, compare Fig. 9-10). Thus, under these conditions the electrochemical system presumably represent a Class II oscillator. For further, prominent experimental systems one should consult the literature on phenomena in semiconductor physics such as the impact-ionization breakdown or the pnpn-diodes where S- and Z- shaped voltammetric profiles are extremely common [227].

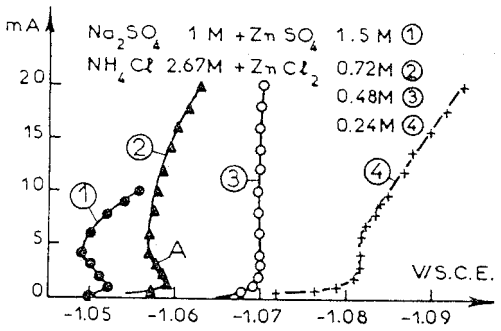

Figure 9-16: Stationary S-shaped I/ϕ profiles for the electrocrystallization of Zn in acidic media at different ionic concentrations (adapted from [240]).

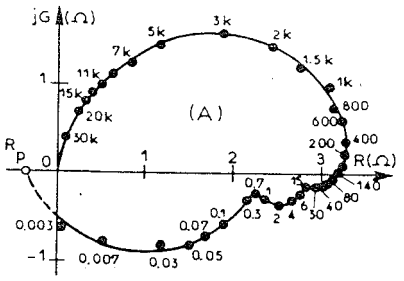

Figure 9-17: Impedance diagram measured at point A of previous figure on the S-shaped polarisation curve (adapted from ref. [240]).

9.3.3 Class III: NDR oscillators

Encompassing some of the most prominent workhorses among electrochemical oscillators, the present mechanistic category is presumably the most wide-spread and, consequently, has been characterized most frequently in the electrochemical literature [74, 23, 242, 32]. Its most crucial features are, first, that the double layer potential ϕ is both an essential and dominant autocatalytic variable owing to a potential region of negative differential resistance along the stationary I/ϕ profile. Purely chemical instabilities are typically absent. Second, but equally important, is the fact that the current oscillations exclusively occur on the stationary I/ϕ branch of negative slope. At vanishing ohmic resistance, the potential region of negative slope naturally yields a monostable N-shaped voltammetric profile (see Fig. 9-1 and Fig. 9-18a). The underlying chemical cause for the negative regulation can be very diverse [73] such as Frumkin double layer effects [18, 71], ad- and desorption of a catalyst [213, 172, 243, 244] or competitive adsorption [73]. Note that the various chemical causes for the negative impedance may imply a varying number of essential species and therefore may influence the number of variables to be considered in modeling.

The indispensable presence of a negative differential resistance has led electrochemists to coin the term NDR-oscillator to denote systems falling into the present category [69, 27, 245]. Fig. 9-18a-c schematically illustrates the cyclovoltammetric behavior of NDR oscillators under strictly potentiostatic, potentiostatic with external resistance and galvanostatic conditions. Obviously, the N-shaped I/ϕ characteristic prevents galvanostatic oscillations, instead it leads always to bistable behavior. Furthermore, as frequently reported in experimental and theoretical studies, the characteristic $U_{ex} - R_{ex}$ bifurcation diagram of NDR oscillators is given by the XPD [44, 71, 64, 74, 72, 27], depicted in Fig. 4-12b. The occurrence of a XPD was ascribed to some inherent symmetry in the relations governing the system dynamics [74], yet has not been completely resolved to date. Directly related to the bifurcation behavior is the characteristic impedance spectrum on the middle I/ϕ branch with negative slope, illustrated in Fig. 9-19. As the ohmic resistance increases, first a Hopf bifurcation is encountered (zero impedance at finite ω) followed by a saddle-node bifurcation beyond a critical R_{ex}. This is another way to illustrate why galvanostatic oscillations are excluded in the present category.

Prototype models pertaining to the NDR category have extensively described in the literature [64, 23, 27].They all include a source term (diffusion, adsorption or reaction) of some slow chemical species (volume or surface species) which subsequently undergoes one or more electrochemical transformations the rate of which shows an N-shaped dependence on potential. From theoretical considerations one can formulate the necessary and sufficient mechanistic ingredients of an NDR oscillator as follows:

- the principal charge-transfer process consists of one or more *dependent* faradaic current carriers with at least one exhibiting an N- shaped I/ϕ profile and
- a slow chemical species- consumed by *all* current carriers - which is formed or transported by a potential-independent process.

Koper indicated the simplest possible formulation of an NDR model writing

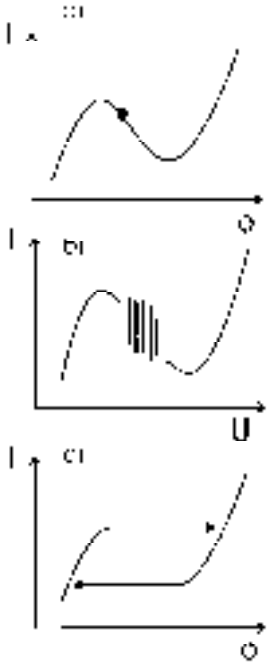

Figure 9-18: Schematic current/potential characteristics for class III (NDR) oscillators: a) strictly potentiostatic I/ϕ behavior with IR compensation; the black solid circle denotes the point associated with the impedance spectrum given in Fig. 9-19, b) potentiostatic I/U behavior for finite ohmic resistances, c) galvanostatic I/ϕ behavior. Arrows, gray areas and bars as in previous figures.

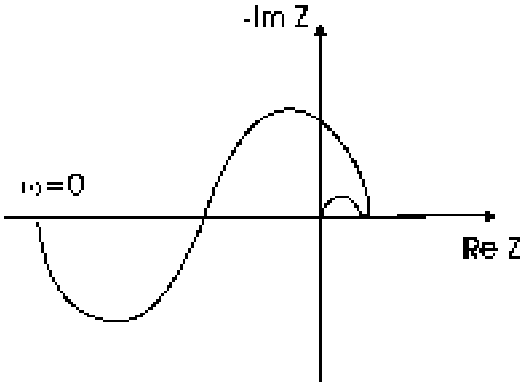

Figure 9-19: Characteristic impedance behavior for class III (NDR) oscillators as measurable at point indicated figure 9-18a.

$$\dot{\theta} = g(\theta) - f(\theta, \phi) \tag{9.17}$$

$$\dot{\phi} = \frac{U_{ex} - \phi}{R_{ex}} - f(\theta, \phi) \tag{9.18}$$

where g and f denote a source term (diffusion/sorption) and a dependent current carrier with N-shaped I/ϕ profile, respectively.

Once an experimental system has been identified as a class III oscillator , $\dot{\theta}/U$ or $\dot{\theta}/I$ feedback tests can help decide whether or not a measurable species shows the appropriate regulation with respect to ϕ (off-diagonal Jacobian sign) in order to comply with the slow negative feedback. It is again noteworthy that the NDR mechanism absolutely allows for multiple faradaic processes as long as all these reactions consume either the slow species or successive intermediates formed by the slow species in the overall process.

Prominent examples of NDR oscillators include the electrodissolution of Fe in sulfuric acid [246], the electrocatalytic reduction of peroxodisulphate on Ag or Pt in acidic media [19, 71] or the reduction of In^{3+} ions in the presence of SCN^- or Cl^- on Hg [66, 70, 247]. Numerous experimental examples of NDR oscillators are found among the electrochemical reduction reaction of anions and of cations in the presence of some catalyst [242] as well as among the systems exhibiting metal electrodissolution around the Flade potential [32, 248, 246, 242]. While in the former systems the N- shaped characteristic arises due to double layer effects and ad-and desorption of the catalyst, respectively, the passivation near the Flade potential provides the negative regulation in the latter systems. Moreover, electrocatalytic oxidation of certain organic fuels such as $HCOH$ on Rh/Ir [115] or ethylene on Pt [112] as well as some electrodeposition reactions are known to belong to class III: Fig. 9-20 displays the typical emergence of current oscillations on the "negative" branch with increasing ohmic resistance in the recently reported electro-codeposition of Cu/Sn in the presence of laprol [216]. Another recently reported example of class III is the H_2O_2 - reduction on Pt and Ag in acidic media at small absolute overpotentials (oscillations referred to as A in ref. [31], more recently [243, 244]). While on Ag the N-shaped stationary I/ϕ profile arises due to an additional, catalyzed reduction pathway by surface species which desorb at higher negative overpotentials, the competitive blockage of catalytic surface sites by adsorbed hydrogen (among other things!) is assumed to be responsible for the negative impedance observed on Pt electrodes.

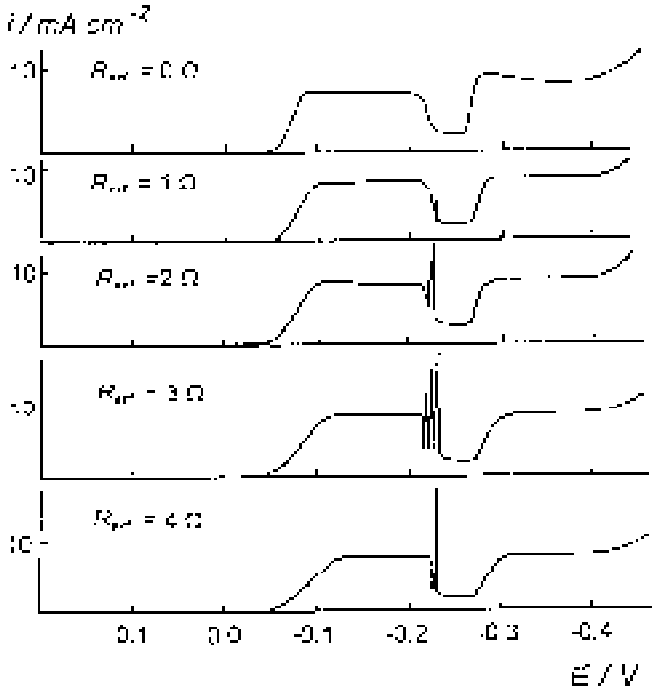

Figure 9-20: Characteristic dependence of the voltammetric profile of class III oscillators on the ohmic resistance as measured during Cu/Sn co-deposition in the presence of laprol 2402S (adapted from ref. [216]).

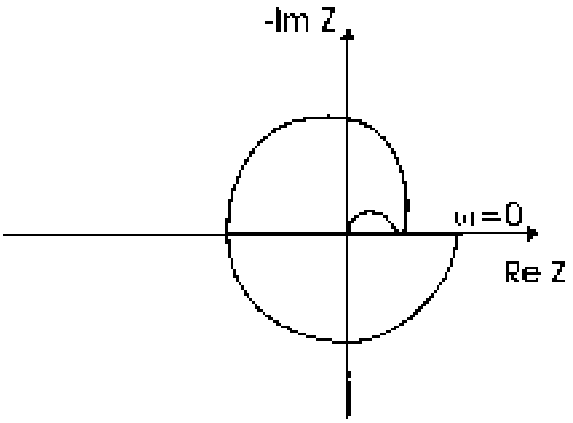

Figure 9-21: Characteristic impedance behavior of class IV (HNDR) oscillators at point indicated in the next figure.

9.3.4 Class IV: HNDR oscillators

The fourth principal oscillator class is related to class III insofar as the double layer potential ϕ is the fast autocatalytic system variable due to a negative differential resistance with chemical species typically providing the slow dynamical feedback. Similarly, potentiostatic current oscillations occur at finite ohmic resistances only. However, in contrast to the preceding class, class IV oscillators usually exhibit current oscillations not only on a I/U branch of negative slope, but most frequently show a HB on a branch with positive regulation, i.e. where the impedance $Z > 0$ [64]. Consequently, a negative differential resistance must be operative on a nonzero timescale, i.e. must be hidden on the stationary polarization curve [64]. Therefore, these oscillators are often referred to as HNDR oscillators [27]. The characteristic feature of a hidden negative impedance is inherently related to two further experimental findings: First, HNDR oscillators display sustained galvanostatic potential oscillations and, second, the typical impedance spectrum measured near the HB resembles the scheme given in Fig. 9-21 [74, 23]. The occurrence of galvanostatic oscillations further implies the absence of a XPD in the $U - R$ bifurcation plot as one Hopf line has to stay "outside" the bistable region for $R \to \infty$.

All experimental features mentioned so far are generally valid for any HNDR oscillator. From mechanistic analyses of numerous HNDR systems, however, it appeared practical to subdivide the HNDR category further into at least three subcategories. Each subcategory exhibits the general features, but on top is characterized by both specific mechanistic and experimental features on which the subdivision is based. It turned out that the prototype models pertaining to the three HNDR subcategories can be derived from the simple NDR model [64] by slight, yet crucial mechanistic modifications. These modifications were initially motivated by the mathematical requirements for galvanostatic oscillations, still allow a plausible translation into chemical terms.

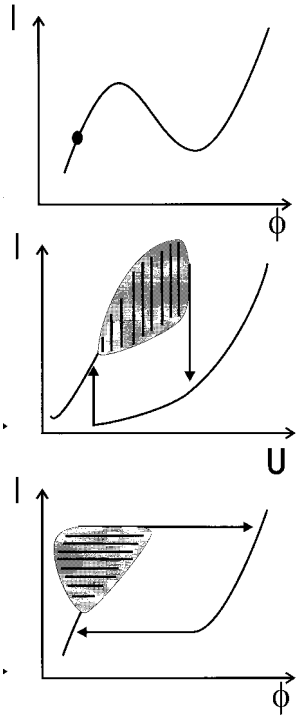

Figure 9-22: Schematic current/potential characteristics of class IV (HNDR) oscillators. a) strictly potentiostatic I/ϕ behavior; the black solid circle denotes the point associated with the impedance spectrum given in the previous figure, b) potentiostatic I/U behavior for finite values of R, c) galvanostatic I/ϕ behavior. Arrows, gray areas and bars as in previous figures.

Class IV.1: Potential-dependent source of the inhibitor

The simplest way to obtain an HNDR oscillator from an NDR model is to assume a potential-dependent source term of the slow, inhibiting species [64]. Starting with eq. 9.17 and 9.18 and assuming a potential dependent adsorption of θ, one can show that the typical voltammetric profile of the HNDR oscillations are recovered. (see Fig. 9-22) The soft transition to sustained oscillations occurs at small absolute overpotentials, while the hard transition (saddle-loop) is observed at large potential values. The additional potential dependence introduces a certain symmetry-breaking [74] (no XPD) which enables galvanostatic oscillations.

Although it appears as a small step from NDR to IV.1, to date there is no experimental example which falls in the IV.1 category.

Class IV.2: The H_2/FA group

This subcategory typically involves an independent current carrier, i.e. a faradaic process consuming nonessential species only; by itself it exhibits a normal potential regulation. Model calculations showed that the current carrier may even be potential-independent (diffusion limited current). As found in most experimental IV.2 systems, the production and removal of an essential chemical species on a fast time scale, here denoted θ_1, modulates the I/ϕ characteristics,e.g. due to surface blocking, such that a N-shaped profile occurs. Finally, a second slow essential chemical species, here denoted θ_2, adds to the mechanism providing the negative feedback. Experimental systems further teach that either the production and/or the removal of θ_2 are potential dependent. Importantly, the dynamics of the slow species covers up the N- shaped profile of the ϕ, θ_1 subsystem such that the HNDR features are obtained just like in the IV.1 case (see Fig. 9-22). It follows that IV.2 systems require three variables for a proper dynamical description, even though - from a mathematical point of view - the ϕ, θ_1 subsystem may be equally replaced by a single evolution equation of ϕ with N-shaped profile. A prototype model and the associated Jacobian sign matrix of a class IV.2 system were described in chapter 7.

It is obvious that a effect of surface blocking of θ_1 can be most easily designed by competitive ad- and desorption where catalytic current carriers are concerned which require free surface sites. Therefore, it is of little surprise that electrocatalytic reaction systems such as H_2 oxidation in the presence of metal cations and anions [29] or the oxidation of organic fuels (see chapter 4 or [215, 242]) fall into this class. Also the nickel dissolution system in the transpassive region can be tentatively classified here [249, 250].

Class IV.3: The IO_3^- group

This subcategory can be derived from an NDR in a pretty simple, straight-forward manner. Adding an appropriate anodic *independent* current carrier to the anodic NDR system (eq. 9.17,9.18) yields the system

$$\dot{\theta} = g(\theta) - f(\theta, \phi) \tag{9.19}$$

$$\dot{\phi} = \frac{U_{ex} - \phi}{R_{ex}} - f(\theta, \phi) - h(\theta, \phi) \tag{9.20}$$

which show the typical general features of an HNDR oscillator. Here, $h(\theta, \phi)$ must not directly consume θ. The additional current providing reaction allows for the total current to be divided among either faradaic process. This adds an additional degree of freedom to the system and allows the recovery of θ at high values of ϕ resulting in galvanostatic limit cycles (see chapter 8 for details). Due to the similar model structure the Jacobian sign matrix of class IV.3 oscillators corresponds to that of class IV.1. However, as pointed out in chapter 8, the bifurcation diagram and voltammetric profiles differ significantly compared to the previous subcategories as the sequence of hard and soft bifurcation to oscillatory behavior is reversed (see Fig.

8-3 and 8-13).

The obvious example for this group is the electrocatalytic IO_3^- reduction system, discussed in chapter 8, as well as related systems such as the $Fe(CN)_6^{3-}$ reduction on Pt [30] or the $Fe(CN)_6^{4-}$ oxidation process [208]. Moreover, the electrocatalytic reduction of $S_2O_8^{2-}$ reduction, on Pt and Ag an NDR system in neutral/alkaline media, "mutates" into a HNDR system in acidic solutions as the hydrogen reduction is shifted to higher potentials overlapping with the $S_2O_8^{2-}$ reduction process. Another recently reported experimental example is the anodic dissolution of Pb-Ag alloy electrodes in acidic sulphate electrodes [217] where oxygen evolution is superimposed on passivating electrode processes leading to a hidden NDR which could be clearly identified by impedance spectroscopy. Finally, the H_2O_2 - reduction system on Pt in acidic solutions at high H_2O_2 concentrations and high negative overpotentials (oscillations B in ref. [31]) is presumably of the IV.3 type, since the N-shaped characteristic at small negative overpotentials (oscillations A in [31]) is superimposed by normally regulated H_2 - evolution. Thus, interestingly, the H_2O_2 - reduction system exhibits both an NDR and a HNDR oscillator in different regions of overpotential due to the same nonlinear feature.

It can not be excluded that the versatile dynamics of the HNDR oscillators can be realized in chemical and mechanistic ways other than illustrated above; this would suggest the introduction of further HNDR subcategories. While IV.3 should be distinguishable on the basis of its bifurcation behavior, IV.1 and IV.2 can be distinguished by their Jacobian sign matrix using feedback control tools (see chapter 7).

9.4 An operational procedure for mechanistic classification

On the basis of the mechanistic characterization and categorization of the preceding sections, it is possible to design a systematic experimental strategy for the classification of unknown electrochemical oscillators. The main purpose of an initial categorization lies in the gain of valuable information on the nature of the essential species, on the roles of individual species and on further mechanistic features such as current carriers etc. From this knowledge the experimenter can start exploring the detailed chemistry with a rather distinct sense of purpose. The following operational procedure is illustrated in Fig. 9-23.

Step 1: Identification of strictly potentiostatic oscillators

The unknown electrochemical oscillator first need to be examined with respect to the existence of sustained current oscillations at vanishing ohmic resistance, i.e. at large electrolyte conductivities. This is necessary since other tests such as impedance spectra do not uniquely specify an oscillator at this point of the classification procedure. In cases where a clear decision remains doubtful, the dynamical I/U feedback control tests as well as the IR compensation technique may help draw clear conclusions. The successful application of the I/U technique proves, whereas the cease of

the oscillations for decreasing R disproves the presence of a class I oscillator. Furthermore, galvanostatic oscillations rule out an electrochemical autocatalysis and $\dot{\theta}/U$ and $\dot{\theta}/I$ control tests of individual, measurable species provide the sign of their potential regulation and help determine their location within the mechanism.

Step 2: Identification of class II oscillators

At this point of the procedure, a S-shaped, bistable strictly potentiostatic profile evidences the presence of some purely chemical bistability. The voltammetric profile may be tested galvanostatically for S or complex S behavior as well as potentiostatically at large resistances. An impedance spectrum similar to Fig. 9-15 should be observable on the middle branch. Then, $\dot{\theta}/U$ and $\dot{\theta}/I$ control tests of the slow, inhibiting species help decide whether the current providing reaction is a dependent or independent current carrier. For example, supposing an electrochemical oxidation system, a dependent (independent) current carrier implies for the Jacobian element $\frac{\partial \dot{\theta}}{\partial \phi} > 0$ ($\frac{\partial \dot{\theta}}{\partial \phi} < 0$).

Step 3: Identification of NDR oscillators

At this stage of the categorization procedure, the impedance spectrum or equivalently the voltammetric profile as well as the U-R bifurcation diagram receive the classification-related impact ascribed to them in ref. [74]. Galvanostatic oscillations definitely rule out an NDR oscillator, whereas bistability unambiguously evidences the presence of the latter. Also, impedance spectra or an XPD can serve as identifying criteria for a class III oscillator. As discussed earlier, the mechanistic variations of NDR systems are pretty much limited to the chemical implementation of the N-shaped characteristics; this usually facilitates the identification of the current carriers or the slow species. Thereafter, a kinetic model can readily be formulated according to the prototype model indicated above.

Step 4: Resolution of the appropriate HNDR class

By default, the electrochemical oscillator under investigation must now belong to the fourth category. Impedance spectra on I/ϕ branches of positive slope as well as cyclovoltammetric data can confirm the default conclusion.

- Step 4.1: Identification of class IV.3

Next, the sequence of the hard and soft bifurcations to limit cycles in the $U_{ex} - R_{ex}$ bifurcation diagram or, more easily, on a single cyclovoltammetric scan (galvanostatic or potentiostatic) need to be considered. The sequence soft transition (supercritical Hopf bifurcation) - hard transition (saddle-loop bifurcation) for increasing absolute overpotentials provides evidence that all dominant current carriers are either dependent or independent, while a reversed sequence suggest the presence of both types of current carriers, i.e. - within our classification scheme - suggests the presence of a IO_3^- group oscillator (class IV.3). In many experimental systems, the slow species is

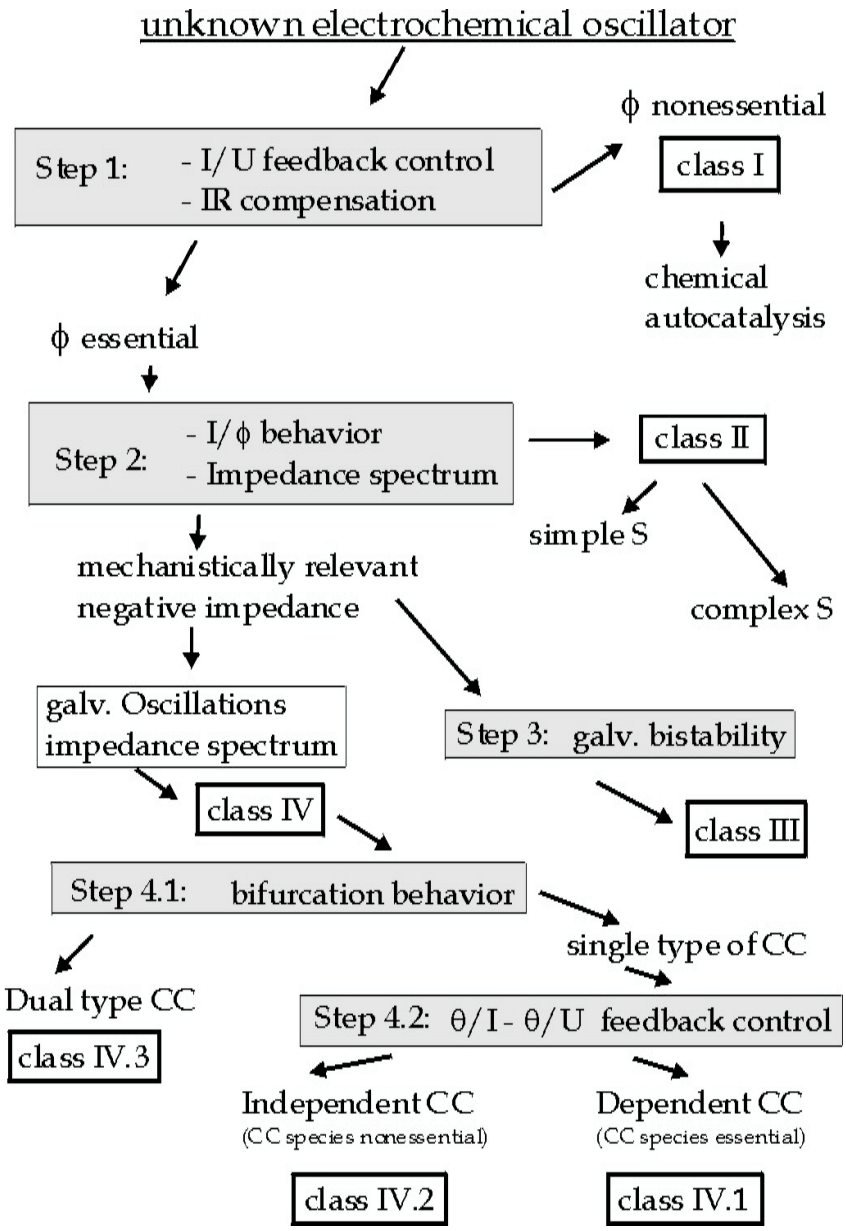

Figure 9-23: Summary of an operational method for the experimental classification of an unknown electrochemical oscillator (CC = current carrier). Details on the experimental procedure are given in the text.

associated with the dominant electroactive reagent, whereas the superimposed additional faradaic process needs to be searched for. The preceding section illustrated an appropriate prototype model applicable for IO_3^- group oscillators.

- Step 4.2: Distinction between class IV.1 and class IV.2

In many experimental oscillators, it is immediately obvious from the electrolyte composition or the experimental conditions whether the dominating faradaic processes are consuming essential or nonessential species, i.e. whether the current carriers are dependent or independent, respectively. If this is not the case, the application of $\dot{\theta}/U$ and $\dot{\theta}/I$ tests using the slow chemical species helps decide the nature of the faradaic process. Conclusions are drawn from the same arguments and relations as mentioned in step 2. If the dominant faradaic process consumes the slow species, obviously a class IV.1 oscillator is present; otherwise the investigated system falls into the IV.2 category. In the latter case, one may need to search for an additional fast species (catalyst, competitive species) exhibiting an inverse potential regulation $\frac{\partial\dot{\theta}}{\partial\phi}$ compared to the slow inhibitor. Here again, the $\dot{\theta}/U$ and $\dot{\theta}/I$ feedback control tests provide a reliable tool in finding appropriate candidates.

9.5 Concluding remarks

In an attempt to reach a practical operational procedure for rapid mechanistic categorization of unknown electrochemical oscillators, the current chapter set off to compile, group and supplement relevant mechanistic and experimental features regarding oscillatory phenomena in electrochemistry.

The categorization scheme required the presence of at least one (electro)chemical autocatalysis in an oscillator's mechanism for the system to be classifiable, thereby excluding the exotic class of nonautocatalytic oscillators. While the principal four classes represent a complete classification scheme, it is not excluded that the introduction of further subcategories may become appropriate in the future.

Emphasis has been placed on the notion of viewing electrochemical oscillators as systems which - to some extent - can be decomposed in individual dynamical functional subunits that, in turn, may be translated in chemical terms. This view obviously suggests a somewhat more dynamics-oriented approach toward the clarification of electrochemical oscillators: the initial assessment of relevant dynamical features, e.g. the category, the role of species, the dynamical nature of faradaic processes, allows a rather directed, subsequent analysis by traditional chemical techniques.

Obviously, for sake of simplicity and clearness the theoretical classification often referred to the simplest and purest realization of an oscillator class possible. Real experimental systems frequently exhibit more complex behavior such as mixed-mode oscillations and/or chaotic behavior [32]. Often this results from the presence of more than one oscillator within the overall chemical mechanism, as exemplified experimentally in the formic acid oxidation (chapter 4 and 5) or, more generally, in the general prototype model for mixed-mode behavior reported in ref. [27] where an NDR and

a HNDR oscillator are superimposed. By appropriate experimental isolation of oscillatory subsystems, however, a single-oscillator classification can yet be performed in these cases.